Reduced Order Modeling and Sliding Mode Control of Active Magnetic Bearing

SUDIPTA SAHA[1]*, (Student Member, IEEE),
SYED MUHAMMAD AMRR[1]*, (Student Member, IEEE),
MASHUQ UN NABI[1], (Member, IEEE),
AND ATIF IQBAL[2], (Senior Member, IEEE)
[1]Department of Electrical Engineering, IIT Delhi, New Delhi 110016, India
[2]Department of Electrical Engineering, Qatar University, Doha, Qatar

Corresponding author: Atif Iqbal (atif.iqbal@qu.edu.qa)

ABSTRACT Due to the accelerated growth in the field of power electronics and controller design techniques, the usage of the active magnetic bearing has picked up in industries. Active magnetic bearing helps the rotor to rotate freely without any physical contact. In brief, this paper develops a model of an active magnetic bearing using the finite element method, and its associated reduced order model, followed by the development of a robust control strategy. COMSOL software is used to perform three-dimensional simulation of an active magnetic bearing system. The state space system matrices are extracted from the finite element method, and a linear time-invariant state-space system is generated in MATLAB. Since the original system is large, the reduced order model is constructed. Then, based upon the reduced order model, a sliding mode control is designed to improve the regulation performance of an active magnetic bearing under unmodeled uncertainties. The stability analysis of closed-loop reduced order model with unmodeled uncertainties guarantees the finite time convergence of system states using Lyapunov theory. Further, it is proved that the same control law will also provide satisfactory performance for the original model using the reduced order model as an observer. The numerical simulation is carried out to illustrate the effective performance of the proposed controller for the reduced model as well as the original model with multiple initial conditions. The proposed work offers an alternative approach of using the reduced order model instead of the original model for the controller design of an active magnetic bearing.

INDEX TERMS Active magnetic bearing, finite element method, full order model, 3D simulation, model order reduction, reduced order model, sliding mode control, finite time convergence.

I. INTRODUCTION

Active magnetic bearing (AMB) is a bearing technology where magnetic forces support the rotor without any physical contact between the rotor and the static support structure. AMB has numerous advantages over conventional bearings like being contactless, lubrication free, wear free, high speed and having reduced vibration [1]–[3]. Due to the development of state-of-art technologies in power electronics domain combined with advances in control algorithms, the application of AMB in the industry has increased.

Along with that, with the rapid advancement of powerful computational tools in recent years, the significance

The associate editor coordinating the review of this article and approving it for publication was Bin Xu.

of numerical simulations has been escalated immensely. There are different numerical techniques for modeling and analysis of AMB like finite element method, finite difference method, boundary element method, etc. In the case of magnetic field analysis in AMB systems, Finite Element Method (FEM) has been preferred [4]–[6] for its flexibility and versatility. The simulation analysis for three and four coil AMB using FEM has been shown in [7]. There exist various FEM software for simulating AMB e.g., COMSOL [8], ANSYS [7], [9], etc. are some of them. In [10], a design procedure and optimization of AMB geometry with the effects of eddy current is presented. The FEM technique converts an inherently distributed parameter system given by partial differential equations (PDE) to a system of ordinary differential equations (ODE). Although ODE is easier to

solve than PDE, due to a large number of ODEs usually encountered in FEM, it gets computationally heavy. Therefore, Model Order Reduction (MOR) [11], [12] is applied in order to reduce the computational burden and to preserve the system properties. The Reduced Order Model (ROM) thus obtained not only decreases the simulation time but also makes controller design easier [13].

On the controller aspects, different types of algorithms have been developed and implemented to control the AMB system over the years. In [14], a hybrid controller based on state feedback approach is developed, and gains are chosen by LQR method. A state based disturbance observer is introduced in [15] for nullifying the mismatched uncertainty. A Kalman estimation based decoupled controller is designed and used for controlling a 5-DOF AMB system in [16]. In [17], an adaptive algorithm for the shaft control of the AMB system has been proposed. A neural network based control has also been applied to the AMB system in [18]. The control of vibrations due to unbalance force has been discussed in [19]. A model predictive based controller is implemented in a single axis AMB system in [20]. For AMB with flexible rotor system, the sliding mode control (SMC) has been designed to nullify the nonlinear effects presented in [21]. Also, in [22], a second-order SMC for the AMB system has been discussed. In the aforementioned papers, only approximate analytic equations are considered for the controller design, whereas in the proposed work, AMB is modeled through FEM to get a realistic model. Then it is reduced to make it suitable for the application of the controller design. Recently, self-sensing AMBs that does not require the use of sensors has also been an active area of research [23]. In this paper, the proposed control strategy also does not require the sensor information.

The main contribution of this work is stated as following:

- Finite element modeling is implemented for AMB using COMSOL software to generate the state-space model. Model order reduction of the generated state-space model is achieved using balanced truncation method.
- The neglected states in the reduction process give rise to the unmodeled dynamics with a known bound. These are taken as uncertainties in the overall control strategy.
- Since the FEM based full order model (FOM) is large, the control strategy involves the designing of the SMC for the reduce order model (ROM), but its implementation is done on the original FOM. The control strategy is shown to be robust to the unmodeled dynamics or uncertainties in the system.
- Moreover, the proposed SMC technique is designed for finite time convergence of ROM states to the origin.
- It is also established that the ROM can act as an observer for the original FOM model, thereby giving the complete state information to the controller rather than one or two positions measured by the sensors. In other words, the control strategy doesn't require the sensor information leading to sensorless control.

This paper is organized as follows: In section II, a brief working principle and FEM modeling of an AMB system

with eddy currents are described. In the next section, balanced truncation based MOR techniques for the AMB system is presented. Section IV discusses the unmodeled dynamics generated due to MOR and its integration in the overall modeling strategies of the AMB. Then in section V, a linear sliding mode control is proposed for ROM to compensate the effects of unmodeled dynamics taken as uncertainties of FOM and the stability analysis is carried out by Lyapunov theorem. In section VI, the applicability of the proposed MOR based control to the original large order system is established. The numerical simulations of the COMSOL model and the performance comparison between FOM and ROM are presented in section VII. Finally, the conclusions are drawn in the last section.

II. WORKING PRINCIPLE & FEM MODELING OF AMB

The essential part of AMB consists of an electromagnet, rotating load, amplifier, a gap sensor, micro-controller, etc. In general, the rotating load levitates with the help of the biased current, which also compensates the weight of the rotor. During the movement of the rotor, if it is dislocated from the central position, then the controller action comes into play. The controller generates a control signal with the help of measurements of the gap sensor. Then power amplifier boosts the control current, and the applied current restores the rotor position. Fig 1 represents a basic diagram of AMB with all components included [24].
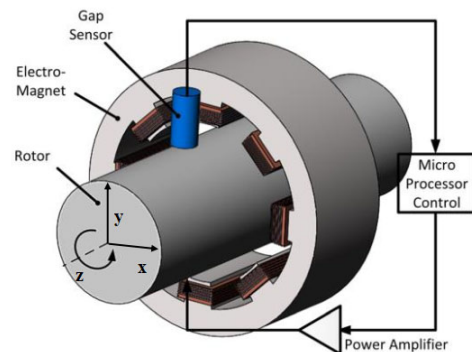

FIGURE 1. Basic diagram of a typical AMB [24].

The FEM modeling of AMB can be classified as in equilibrium point and displaced position. The equilibrium position refers to the undisturbed position of AMB, where the rotor rotates without any axial vertical displacement, and the controller remains idle. The total input current in the model consists of bias current I_0 and control current I_y. First, we describe the modeling of AMB for the equilibrium position. The magnetic flux density in equilibrium can be written as $\hat{B}_0 = curl\ \hat{A}_0$, where $\hat{A}_0$ is the magnetic vector potential and $\hat{B}_0$ is magnetic flux density due to bias current I_0. The $curl\ \hat{A}_0$ is defined as:

$$curl\ \hat{A}_0 = \begin{vmatrix} i & j & k \\ \frac{\partial}{\partial x} & \frac{\partial}{\partial y} & \frac{\partial}{\partial z} \\ \hat{A}_{0,x} & \hat{A}_{0,y} & \hat{A}_{0,z} \end{vmatrix}. \qquad (1)$$

The electromagnetic behavior of AMB is defined by Poisson's equation

$$curl\left(\frac{1}{\mu}curl\,\hat{A}_0\right)=\sigma\left(\frac{\partial\hat{A}_0}{\partial t}\right)+J_0, \tag{2}$$

where μ is magnetic permeability, σ is electrical conductivity and J_0 is the current density due to the bias current. The generated force from the magnetic flux density in equilibrium can be given using Maxwell stress tensor as [25], where n is the unit outward normal vector of the integration surface S

$$F_0=\int_s\left(\frac{1}{\mu_0}\left(\hat{B}_0\cdot n\right)\hat{B}_0-\frac{1}{2\mu_0}\hat{B}_0^2 n\right)dS. \tag{3}$$

The magnetic flux density is dependent on the control current I_y and displacement y. Therefore, generated force also becomes a function of I_y and y. The generated force helps the rotor to stay in equilibrium position by balancing the load as

$$F_0=mg, \tag{4}$$

where m is the mass of the rotor and g is the gravity.

The modeling of AMB for the general displaced position is presented next. The entire analysis of AMB is considered to be linear. The magnetic flux density in displaced position can be given as $\hat{B}=\hat{B}_0+\hat{B}_y=curl\,(\hat{A}_0+\hat{A}_y)$, where $\hat{A}_y$ is the magnetic vector potential and $\hat{B}_y$ is the magnetic flux density due to an impressed control current density J_y, corresponding to an input control current I_y. For the displaced position electromagnetic behavior is defined as

$$curl\left(\frac{1}{\mu}curl\,(\hat{A}_0+\hat{A}_y)\right)=\sigma\left(\frac{\partial(\hat{A}_0+\hat{A}_y)}{\partial t}\right)+J_0+J_y. \tag{5}$$

The generated force can be presented as [25]

$$F=F_0+F_y=\int_s\left(\frac{1}{\mu_0}\left(\hat{B}\cdot n\right)\hat{B}-\frac{1}{2\mu_0}\hat{B}^2 n\right)dS. \tag{6}$$

The motion of the rotor around y axis is defined as below

$$F=mg+m\frac{d^2y}{dt^2}=F_0+m\frac{d^2y}{dt^2}. \tag{7}$$

The bias current nullifies the weight mg of the AMB system and control current helps for the dynamic movement of this system. Now, subtracting out the equilibrium conditions (2), (3) and (4) from the total expressions (5), (6) and (7), we get the equation for displaced state of the rotor as

$$curl\left(\frac{1}{\mu}curl\,\hat{A}_y\right)=\sigma\left(\frac{\partial\hat{A}_y}{\partial t}\right)+J_y, \tag{8}$$

$$F_y=\int_s\left(\frac{1}{\mu_0}\left(\hat{B}_y\cdot n\right)\hat{B}_y-\frac{1}{2\mu_0}\hat{B}_y^2 n\right)dS, \tag{9}$$

$$F_y=m\frac{d^2y}{dt^2}. \tag{10}$$

Recalling that AMB is an electro-mechanical device, the electromagnetic and mechanical models can be picturized
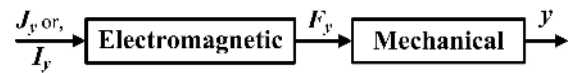

FIGURE 2. Basic structure of AMB.

as shown in Figure 2 to obtain the overall model. The electromagnetic block in Figure 2 is governed by (8) and (9), both being PDE's, while the mechanical block is governed by (10), which is a single ordinary differential equation.

The FEM model generated from applying FEM method to (8), (9) leads to a system of differential algebraic equations (DAE's). Some of the equations in these DAE's are purely algebraic equations that correspond to parts where there is no conductor. In parts of the domain which contain conducting regions, differential equations arise. The purely algebraic equations can be eliminated without much computational effort by one of the techniques reported in [26], [27]. Alternatively, software like COMSOL has inbuilt features which converts the DAE's to ODE's. In either case, these DAE's can be converted to the system of ODE's. Together with (10), they are given as

$$\bar{E}\dot{\mathbf{x}}(t)=\bar{A}\mathbf{x}(t)+\bar{B}u(t);\quad \mathbf{x}(0)=\mathbf{x}_0, \tag{11}$$

$$\mathbf{y}=\bar{C}\mathbf{x}(t), \tag{12}$$

where $\bar{E}\in\mathbb{R}^{n\times n},\bar{A}\in\mathbb{R}^{n\times n},\bar{B}\in\mathbb{R}^{n\times m},\bar{C}\in\mathbb{R}^{p\times n},x(t)\in\mathbb{R}^n,x_0\in\mathbb{R}^n,u(t)\in\mathbb{R}^m$. The system has m input, p output and order n, where n denotes number of nodes in the conducting regions usually a large number. In this case, $m=1$ and $p=1$. The input u in the model is control current I_y and output is displacement from central position y. Moreover, $\bar{E}$ and $\bar{A}$ are sparse, invertible and symmetric matrices. As DAE's converted to ODE's after elimination of most of the algebraic states, FEM model is converted to sparse system. Invertible and symmetric matrices are obtained because the generated system is stable. The number n still being in the thousands, the model (11) & (12), referred to as the Full Order Model (FOM), is then reduced using MOR technique. It should be noted that since $\bar{E}$ is nonsingular, hence (11) & (12) can also be put in the normal state space form, given as

$$\tilde{A}=\bar{E}^{-1}\bar{A},\quad \tilde{B}=\bar{E}^{-1}\bar{B},\ \tilde{C}=\bar{C}. \tag{13}$$

However, doing this would destroy the sparsity of the model and hence is avoided, practically for computational difficulties.

III. REDUCED ORDER MODELING OF AMB

It is difficult to simulate and analyze large order models and designing a controller for such systems is also very difficult. In order to accomplish these tasks, it is essential to convert the large order systems to smaller order systems. Model order reduction is a tool to convert large order models to much smaller order models while capturing necessary dynamical behaviors and properties of the original large order models.

To reduce the system, we have used balanced truncation, which is a popular method for model order reduction.

Balanced truncation not only preserves some of the important system properties, but it also keeps the reduction error at a bound [28]. In order to use balanced truncation, we need the controllability and observability Gramians W_c and W_o, respectively, which can generally be expressed as

$$W_c = \int_0^\infty e^{A\tau} BB^T e^{A^T\tau} d\tau, \tag{14}$$

$$W_o = \int_0^\infty e^{A^T\tau} C^T C e^{A\tau} d\tau. \tag{15}$$

It is noted that both W_c and W_o are positive definite. After getting W_c, W_o from (14) and (15) singular value decomposition of the product can be represented as

$$W_c W_o = U\Sigma T^T, \tag{16}$$

where U and T are respectively the left and right singular vectors and Σ is the diagonal matrix containing the singular values $\sigma_1, \sigma_2, ..., \sigma_n$. Based on magnitude, the singular values are partitioned into $\Sigma_1 = \sigma_1, \sigma_2, \ldots, \sigma_q$ and $\Sigma_2 = \sigma_{q+1}, \ldots, \sigma_n$. The singular vectors U and V are also partitioned accordingly. Balanced truncation keeps the singular values in Σ_1 and throws away the singular values in Σ_2.

Computationally, controllability and observability Gramians W_c and W_o are given by solutions X and Y of the generalized Lyapunov equations

$$\bar{A}X\bar{E}^T + \bar{E}X\bar{A}^T + \bar{B}\bar{B}^T = 0, \tag{17}$$

$$\bar{A}^T Y\bar{E} + \bar{E}^T Y\bar{A} + \bar{C}^T\bar{C} = 0, \tag{18}$$

where

$$W_c = X, \qquad W_o = \bar{E}^T Y\bar{E}. \tag{19}$$

The above generalized Lyapunov equations are computationally heavy. But they can be solved through various ways which involves less computation [29]–[31]. If we consider a generalized Lyapunov equation as

$$\bar{A}^T X\bar{E} + \bar{E}^T X\bar{A} + N = 0, \tag{20}$$

then, the solution of the above equation can be obtained as in [31]. Equation (18) can be computed from (20) by setting $N = \bar{C}^T\bar{C}$. Equation (17) can be computed from (20) by changing iteration of A to A^T, and setting $N = \bar{B}\bar{B}^T$. Then the Gramians W_c and W_o can be calculated by the method given in [32].

After getting symmetric and positive semi-definite W_c and W_o from (19), Cholesky factorizations can be calculated as below

$$W_c = KK^T, \quad W_o = LL^T. \tag{21}$$

Using these factors, the singular value decomposition can be evaluated as [33]

$$L^T\bar{E}K = \begin{bmatrix} U_1 & U_2 \end{bmatrix} \begin{bmatrix} \Sigma_1 & 0 \\ 0 & \Sigma_2 \end{bmatrix} \begin{bmatrix} T_1^T \\ T_2^T \end{bmatrix}, \tag{22}$$

where $\Sigma_1 \in \mathbb{R}^{q\times q}$ reflects dominant singular values, also called the dominant Hankel singular values of the system (11) and (12). The projection matrices are created as

$$W = LU_1\Sigma_1^{-\frac{1}{2}} \quad \text{and} \quad V = KT_1\Sigma_1^{-\frac{1}{2}}. \tag{23}$$

Then the reduced order model is computed as

$$\begin{aligned} \bar{E}_q &= W^T\bar{E}V, \\ \bar{A}_q &= W^T\bar{A}V, \\ \bar{B}_q &= W^T\bar{B}, \\ \bar{C}_q &= \bar{C}V. \end{aligned} \tag{24}$$

MOR generates a Reduced Order Model (ROM) of order $q \ll n$ such that input-output characteristics and other important information are preserved. The original model is reduced to a much smaller order system via balanced truncation, so the value of q will be much less than n. The reduced order model can be represented as (25) and (26) where $\mathbf{x}_q \in \mathbb{R}^q$

$$\bar{E}_q\dot{\mathbf{x}}_q(t) = \bar{A}_q\mathbf{x}_q(t) + \bar{B}_q u(t); \quad \bar{\mathbf{x}}(0) = \bar{\mathbf{x}}_0, \tag{25}$$

$$\mathbf{y} = \bar{C}_q\mathbf{x}_q(t), \tag{26}$$

where $\bar{E}_q \in \mathbb{R}^{q\times q}, \bar{A}_q \in \mathbb{R}^{q\times q}, \bar{B}_q \in \mathbb{R}^{q\times m}, \bar{C}_q \in \mathbb{R}^{p\times q}$. Note that for the reduced system $\bar{E}_q$ can be expressed as

$$\begin{aligned} \bar{E}_q = W^T\bar{E}V &= \Sigma_1^{-\frac{1}{2}} U_1^T L^T\bar{E}KT_1\Sigma_1^{-\frac{1}{2}}, \\ &= \Sigma_1^{-\frac{1}{2}} U_1^T U_1\Sigma_1 T_1^T T_1\Sigma_1^{-\frac{1}{2}}, \\ &= \Sigma_1^{-\frac{1}{2}} \Sigma_1\Sigma_1^{-\frac{1}{2}}, \\ \bar{E}_q &= I_{q\times q}. \end{aligned} \tag{27}$$

MOR achieved through balanced truncation keeps the dominant states and throws away the less dominant states. The deducted states give unmodeled dynamics that can be taken as an uncertainty in the controller design procedure.

IV. INTEGRATION OF ROM AND UNMODELED DYNAMICS IN MODELING OF AMB

It should be noted that balanced truncation model reduction strategy seeks to capture the controllable and observable states only while throwing away the uncontrollable and unobservable dynamics. Mathematically, we truncate the states based on dominant singular values. Therefore, the unmodeled dynamics consisting of relatively uncontrollable and unobservable states is related to the truncated Hankel values $\sigma_{q+1}, \sigma_{q+2}, ..., \sigma_n$. Generally, the bound of the uncertainty in the unmodeled dynamics can be obtained and given by Hankel norm error as [34], [35]

$$\|G(s) - G_q(s)\|_\infty \leq 2(\sigma_{q+1} + \sigma_{q+2} + ... + \sigma_n), \tag{28}$$

where $G(s)$ is the transfer function of the original model, and $G_q(s)$ is the transfer function of the reduced model.

Now in the present case, the overall system is given as in Figure 3, which can be related to Figure 2 as well. The first dotted subsystem in Figure 3 is the electromagnetic part with the transfer function G_1, and I_y and F_y are the control input
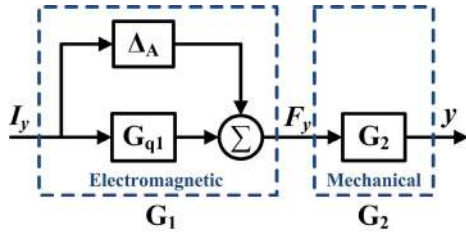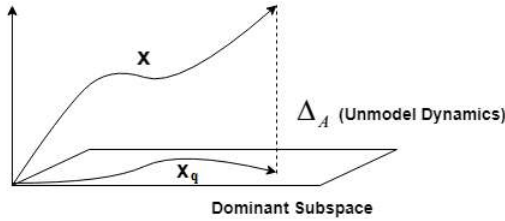
FIGURE 3. Overall transfer function.

FIGURE 4. Relation between ROM and FOM.

current and output force, respectively. The transfer function G_1 comprises of G_{q1} representing the ROM and Δ_A describing the unmodeled dynamics. The second dotted subsystem is the mechanical part with G_2 being the transfer function, and y is the axial displacement of the rotor from the central position.

The overall transfer function G from Figure 3 is given as

$$G = (G_{q1} + \Delta_A) \cdot G_2. \tag{29}$$

Since no MOR is involved in $G_2 = \frac{1}{ms^2}$, which is completely known, the effect of ROM is only that some part of the dynamics of G_1 is lost. The lost dynamics is considered as the uncertainty Δ_A. In other words, Δ_A is the sum total of all the unmodeled dynamics that has been thrown away in the MOR process (Figure 4).

$$G_1 = G_{q1} + \Delta_A. \tag{30}$$

The boundedness of uncertainty Δ_A can be shown from (28) and (30) as

$$\Delta_A = G_1 - G_{q1}, \tag{31}$$

$$\|\Delta_A\|_\infty = \|G_1 - G_{q1}\|_\infty, \tag{32}$$

$$\|\Delta_A\|_\infty \le 2(\sigma_{q+1} + \sigma_{q+2} + \ldots + \sigma_n), \tag{33}$$

or,

$$\|\Delta_A(j\omega)\|_\infty \le \hat{Z}, \qquad \forall \omega, \tag{34}$$

where ω is the angular frequency and $\hat{Z}$ is the upper bound, which is scalar. Hence, (30) can be written as [36]

$$G_1 \le G_{q1} + \hat{Z}\Delta, \tag{35}$$

where Δ is a transfer function satisfying $|\Delta| \le 1$ for all ω.

V. DESIGN OF PROPOSED SMC
In this section, the control law is designed for the reduced order system. The inequality of (35) is removed to consider the worst case when the uncertainty is equal to the upper bound (i.e., $\hat{Z}$). If the proposed control law works for the

worst case, then it is obvious that it will work for any other instances in which the uncertainty is less than $\hat{Z}$. The reduced order system in state space is defined as

$$\dot{\mathbf{x}}_q = \bar{A}_q \mathbf{x}_q + \bar{B}_q u + \delta, \tag{36}$$

where $\delta \in \mathbb{R}^{q \times 1}$ represents the uncertainties due to the neglected part of the original system in ROM. The following remarks are considered while designing the control law.

Remark 1: The upper bound of δ is known, which satisfies $\|\delta(t)\|_\infty = \|\mathcal{L}^{-1}[\Delta_A(j\omega)]\|_\infty \le Z$ from (34) where $\mathcal{L}^{-1}[.]$ is the inverse Laplace transform of the unknown uncertainties $\Delta_A(j\omega)$. Furthermore, the ROM of order q from (36) obtained using balanced truncation method is controllable and observable.

Now the reduced order system (36) is converted into a controllable canonical form by using a transformation matrix $P \in \mathbb{R}^{q \times q}$ which is constructed from the eigenvectors of $\bar{A}_q$ as

$$\tilde{\mathbf{x}}_q = P^{-1}\mathbf{x}_q \quad \text{or,} \quad \mathbf{x}_q = P\tilde{\mathbf{x}}_q, \tag{37}$$

where $\tilde{\mathbf{x}}_q \in \mathbb{R}^q$. By substituting the value of $\mathbf{x}_q$ from (37) into (36) and rewritten in terms of $\tilde{\mathbf{x}}_q$ yields

$$P\dot{\tilde{\mathbf{x}}}_q = \bar{A}_q P\tilde{\mathbf{x}}_q + \bar{B}_q u + \delta,$$
$$\dot{\tilde{\mathbf{x}}}_q = P^{-1}\bar{A}_q P\tilde{\mathbf{x}}_q + P^{-1}\bar{B}_q u + P^{-1}\delta,$$
$$\dot{\tilde{\mathbf{x}}}_q = \underbrace{P^{-1}\bar{A}_q P}_{\tilde{A}_q}\tilde{\mathbf{x}}_q + \underbrace{P^{-1}\bar{B}_q}_{\tilde{B}_q} u + \underbrace{P^{-1}\delta}_{\tilde{\delta}},$$
$$\dot{\tilde{\mathbf{x}}}_q = \tilde{A}_q\tilde{\mathbf{x}}_q + \tilde{B}_q u + \tilde{\delta}, \tag{38}$$

where $\tilde{A}_q \in \mathbb{R}^{q \times q}$ and $\tilde{B}_q \in \mathbb{R}^{q \times 1}$ are the reduced order system matrix in the canonical form which are expressed as

$$\tilde{A}_q = \begin{bmatrix} 0 & 1 & 0 & \cdots & 0 \\ 0 & 0 & 1 & \cdots & 0 \\ \vdots & \vdots & \ddots & \ddots & 0 \\ 0 & 0 & 0 & \cdots & 1 \\ -a_1 & -a_2 & -a_3 & \cdots & -a_q \end{bmatrix}; \quad \tilde{B}_q = \begin{bmatrix} 0 \\ 0 \\ \vdots \\ 0 \\ 1 \end{bmatrix}, \tag{39}$$

and the term $\tilde{\delta}$ is the uncertainty in the canonical form defined as

$$\tilde{\delta} = \begin{bmatrix} w_1 & w_2 & \cdots & w_{q-1} & w_q \end{bmatrix}^T. \tag{40}$$

Hence, the reduced order system in (36) is now transformed into canonical form as given in (38). The canonical form (38) can also be expressed as

$$\dot{\tilde{x}}_1 = \tilde{x}_2 + w_1,$$
$$\dot{\tilde{x}}_2 = \tilde{x}_3 + w_2,$$
$$\vdots$$
$$\dot{\tilde{x}}_{q-1} = \tilde{x}_q + w_{q-1},$$
$$\dot{\tilde{x}}_q = -a_1\tilde{x}_1 - a_2\tilde{x}_2 - \cdots - a_q\tilde{x}_q + u + w_q, \tag{41}$$

where $\tilde{x}_i$ for $i = 1, 2, \ldots, q$, are the individual states of vector $\tilde{\mathbf{x}}_q$.

A linear sliding surface $s \in \mathbb{R}$ is designed by a linear combination of system states as

$$s = c_1 \tilde{x}_1 + c_2 \tilde{x}_2 + \cdots + c_{q-1} \tilde{x}_{q-1} + \tilde{x}_q, \quad (42)$$
$$\text{or,} \quad s = \Upsilon^T \tilde{\mathbf{x}}_q, \quad (43)$$

where $\Upsilon = [c_1, c_2, \cdots, c_{q-1}, 1]^T$ and c_i are all positive design parameter constants. Differentiating (42) will give

$$\dot{s} = c_1 \dot{\tilde{x}}_1 + c_2 \dot{\tilde{x}}_2 + \cdots + c_{q-1} \dot{\tilde{x}}_{q-1} + \dot{\tilde{x}}_q. \quad (44)$$

Now putting the values of $\dot{\tilde{x}}_i$ from (41) in (44) yields

$$\dot{s} = c_1 \tilde{x}_2 + c_2 \tilde{x}_3 + \cdots + c_{q-1} \tilde{x}_q + (-a_1 \tilde{x}_1 - a_2 \tilde{x}_2 - \cdots \\ \cdots - a_q \tilde{x}_q + u + w_q) + c_1 w_1 + c_2 w_2 + \cdots + c_{q-1} w_{q-1}, \quad (45)$$

$$\dot{s} = (0 - a_1) \tilde{x}_1 + (c_1 - a_2) \tilde{x}_2 + \cdots + (c_{q-2} - a_{q-1}) \tilde{x}_{q-1} \\ + (c_{q-1} - a_q) \tilde{x}_q + c_1 w_1 + c_2 w_2 + \cdots + c_{q-1} w_{q-1} \\ + w_q + u. \quad (46)$$

The proposed SMC is the combination of equivalent control u_{eq} and switching control u_{sw}. Therefore, the total control u is given as

$$u = u_{eq} + u_{sw}. \quad (47)$$

The equivalent and switching control are selected as

$$u_{eq} = [-\{(-a_1) \tilde{x}_1 + (c_1 - a_2) \tilde{x}_2 + (c_2 - a_3) \tilde{x}_3 + \cdots \\ + (c_{q-1} - a_q) \tilde{x}_q\}], \quad (48)$$
$$u_{sw} = [-c_1 \bar{w} - c_2 \bar{w} - \cdots - c_{q-1} \bar{w} - \bar{w}] \, \text{sgn}(s) - \eta \, \text{sgn}(s) \quad (49)$$

where $\bar{w}$ is the upper bound of uncertainties w_i i.e.,

$$|w_i| \leq \bar{w}, \quad (50)$$

and η is a positive gain constant. The following theorem proves the finite time convergence of system states.

Theorem 1: Consider the reduced order system in canonical form (41) under Remark 1 and a linear sliding surface (42). The proposed SMC (47) with equivalent and switching controls (48) & (49), respectively will converge the system states $\tilde{\mathbf{x}}_q$ to their equilibrium points in a finite time.

Proof: Consider a Lyapunov function candidate $\mathcal{V}_1$ as

$$\mathcal{V}_1 = \frac{1}{2} s^2. \quad (51)$$

The time derivative of (51)

$$\dot{\mathcal{V}}_1 = s \dot{s}. \quad (52)$$

Substituting the value of $\dot{s}$ from (46) in (52) yields

$$\dot{\mathcal{V}}_1 = s\{(-a_1) \tilde{x}_1 + (c_1 - a_2) \tilde{x}_2 + (c_2 - a_3) \tilde{x}_3 + \cdots \\ + (c_{q-1} - a_q) \tilde{x}_q + \sum_{i=1}^{q-1} c_i w_i + w_q + u\}. \quad (53)$$

After putting the value of u from (47) in (53) yields

$$\dot{\mathcal{V}}_1 = s \left[\sum_{i=1}^{q-1} c_i w_i + w_q + u_{sw} \right]. \quad (54)$$

Now substituting the value of u_{sw} from (49) into (54) will give

$$\dot{\mathcal{V}}_1 = c_1 w_1 s + c_2 w_2 s + \cdots + c_{q-1} w_{q-1} s + w_q s \\ - c_1 \bar{w} s \, \text{sgn}(s) - c_2 \bar{w} s \, \text{sgn}(s) - \cdots - c_{q-2} \bar{w} s \, \text{sgn}(s) \\ - c_{q-1} \bar{w} s \, \text{sgn}(s) - \bar{w} s \, \text{sgn}(s) - \eta s \, \text{sgn}(s), \\ = c_1 w_1 s + c_2 w_2 s + \cdots + c_{q-1} w_{q-1} s + w_q s - c_1 \bar{w} |s| \\ - c_2 \bar{w} |s| - \cdots - c_{q-1} \bar{w} |s| - \bar{w} |s| - \eta |s|, \\ \leq c_1 |w_1| |s| + c_2 |w_2| |s| + \cdots + c_{q-1} |w_{q-1}| |s| \\ + |w_q| |s| - c_1 \bar{w} |s| - c_2 \bar{w} |s| - \cdots - c_{q-1} \bar{w} |s| \\ - \bar{w} |s| - \eta |s|, \\ \leq -c_1 |s| (\bar{w} - |w_1|) - c_2 |s| (\bar{w} - |w_2|) - \cdots \\ - c_{q-1} |s| (\bar{w} - |w_{q-1}|) - |s| (\bar{w} - |w_q|) - \eta |s|. \quad (55)$$

Since $\bar{w} \geq |w_i|$ from (50), therefore $\dot{\mathcal{V}}_1$ in (55) can be further upper bounded as

$$\dot{\mathcal{V}}_1 \leq -\eta |s|, \\ \leq -\sqrt{2} \, \eta \mathcal{V}_1^{\frac{1}{2}}, \\ \dot{\mathcal{V}}_1 \leq -\alpha \mathcal{V}_1^{\frac{1}{2}}, \quad (56)$$

where $\alpha = \sqrt{2} \, \eta > 0$ and $\mathcal{V}_1$ is positive definite, therefore, $\dot{\mathcal{V}}_1$ is negative definite. So, according to finite time convergence lemma given in [37], it can be concluded that since the time derivative of $\mathcal{V}_1$ is in the form of (56), therefore the sliding surface s will converge to zero in a finite time. Moreover, s is a linear combination of states $\tilde{\mathbf{x}}_q$ as defined in (43), therefore ROM states $\tilde{x}_i$ for $i = 1, 2, \ldots, q$, will also converge to their equilibrium points in a finite time. This completes the proof of finite time convergence of system states under the action of proposed SMC. Moreover, the same controller will also perform satisfactorily with finite time convergence in the worst case scenario where the uncertainties will be at its upper bound.

The subsequent section describes the feasibility of the proposed controller (47) for the original system.

VI. IMPLEMENTATION OF PROPOSED CONTROLLER TO FOM

The proposed controller (47) is designed under the consideration of ROM under Remark 1. But, a similar controller design analysis for FOM is not feasible, since most of its states are uncontrollable and unobservable. Therefore, for performance comparison, the implementation of the proposed controller to both ROM and FOM is not straightforward. The proposed SMC is applied to both ROM and FOM according to the closed loop block diagram given in Figure 5. In Figure 5, the ROM is considered to be acting as an observer model for FOM. Therefore, the same closed loop control, which is obtained from the closed loop feedback of ROM is applied
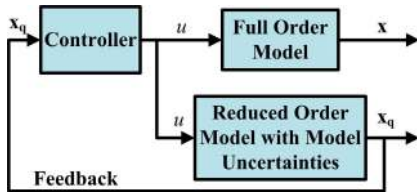
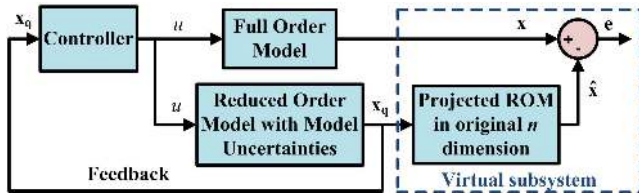**FIGURE 5.** Block diagram of proposed control system for ROM.

FIGURE 6. Block diagram of proposed control for performance analysis between ROM and FOM.

to FOM. Now, the convergence of error between FOM and ROM system states is proved in the next theorem according to Figure 6. The dotted part in Figure 6 represents the virtual system to carry out the theoretical analysis of the error dynamics. The signals $\mathbf{x}$ and $\hat{\mathbf{x}}$ are the non-physical signals. For theoretical analysis, the original FOM can be taken as the standard state space form given in (13). In the proof, the following property is used.

Property 1 *[38]:* The negative-definite and symmetric system matrix A satisfies the following condition for any vector $\mathbf{v} = [v_1 \ v_2 \ v_3]^T \in \mathbb{R}^3$:

$$\lambda_{\min}(A) \|\mathbf{v}\|^2 \le \mathbf{v}^T A \mathbf{v} \le \lambda_{\max}(A) \|\mathbf{v}\|^2, \tag{57}$$

where $\lambda_{\max}(A)$ and $\lambda_{\min}(A)$ are the maximum and minimum eigen values of A, respectively.

Theorem 2: Under *Remark 1*, consider the dynamics of FOM (13) and ROM (36). With the closed loop strategy given in Figure 6 under the action of the proposed controller (47), the error between the states of FOM and the projected ROM in original order space will uniformly converge to a narrow bound in the neighborhood of zero.

Proof: The reduced order system states $\mathbf{x}_q$ from (36) can be transformed to the original order space of dimension n by multiplying the projection matrix $V \in \mathbb{R}^{n \times q}$ as expressed in (58)

$$V\mathbf{x}_q = \hat{\mathbf{x}} \text{ or, } \mathbf{x}_q = V^T \hat{\mathbf{x}}. \tag{58}$$

Now the reduced order system is transformed into the original order space, but this does not mean it is the same as original FOM. The reduced order system given by (36) can be rewritten as

$$\begin{aligned} I_{q \times q} \dot{\mathbf{x}}_q &= \bar{A}_q \mathbf{x}_q + \bar{B}_q u + \boldsymbol{\delta}, \\ V \dot{\mathbf{x}}_q &= V(\bar{A}_q \mathbf{x}_q + \bar{B}_q u + \boldsymbol{\delta}), \\ \dot{\hat{\mathbf{x}}} &= V\bar{A}_q \mathbf{x}_q + V\bar{B}_q u + V\boldsymbol{\delta}, \\ \dot{\hat{\mathbf{x}}} &= V\bar{A}_q V^T \hat{\mathbf{x}} + V\bar{B}_q u + V\boldsymbol{\delta}, \\ \dot{\hat{\mathbf{x}}} &= \check{A}_q \hat{\mathbf{x}} + \check{B}_q u + V\boldsymbol{\delta}, \end{aligned} \tag{59}$$

where $\hat{\mathbf{x}} \in \mathbb{R}^n$, $\check{A}_q = V\bar{A}_q V^T \in \mathbb{R}^{n \times n}$, $\check{B}_q = V\bar{B}_q \in \mathbb{R}^{n \times 1}$.

The error between the states of original system $\mathbf{x}$ and transformed reduced system $\hat{\mathbf{x}}$ is expressed as

$$\mathbf{e} = \mathbf{x} - \hat{\mathbf{x}}. \tag{60}$$

Substituting the dynamics of FOM (13) and transformed ROM (59) into the time derivative of error (60) yields

$$\begin{aligned} \dot{\mathbf{e}} &= \dot{\mathbf{x}} - \dot{\hat{\mathbf{x}}}, \\ &= \tilde{A}\mathbf{x} + \tilde{B}u - (\check{A}_q \hat{\mathbf{x}} + \check{B}_q u + V\boldsymbol{\delta}), \\ &= \tilde{A}(\mathbf{e} + \hat{\mathbf{x}}) - \check{A}_q \hat{\mathbf{x}} + (\tilde{B} - \check{B}_q)u - V\boldsymbol{\delta}, \\ &= \tilde{A}\mathbf{e} + \underbrace{(\tilde{A} - \check{A}_q)\hat{\mathbf{x}} + (\tilde{B} - \check{B}_q)u}_{\Phi} - V\boldsymbol{\delta}, \end{aligned} \tag{61}$$

where $\Phi \in \mathbb{R}^{n \times 1}$ is the difference between FOM and ROM defined as

$$\Phi = (\tilde{A} - \check{A}_q)\hat{\mathbf{x}} + (\tilde{B} - \check{B}_q)u. \tag{62}$$

The equation (61) can be rewritten as

$$\dot{\mathbf{e}} = \tilde{A}\mathbf{e} + \underbrace{\Phi - V\boldsymbol{\delta}}_{\Gamma}$$

$$\dot{\mathbf{e}} = \tilde{A}\mathbf{e} + \Gamma. \tag{63}$$

To show the convergence of $\mathbf{e}$ in the vicinity of zero, lets consider another Lyapunov candidate $\mathcal{V}_2$

$$\mathcal{V}_2 = \frac{1}{2}\mathbf{e}^T \mathbf{e}. \tag{64}$$

Taking the time derivative of (64) and using the Property 1

$$\begin{aligned} \dot{\mathcal{V}}_2 &= \mathbf{e}^T \dot{\mathbf{e}}, \tag{65} \\ &= \mathbf{e}^T(\tilde{A}\mathbf{e} + \Gamma), \\ &= \mathbf{e}^T \tilde{A}\mathbf{e} + \mathbf{e}^T \Gamma, \\ &\le \underbrace{\lambda_m(\tilde{A})}_{-k} \|\mathbf{e}\|^2 + \|\mathbf{e}\| \|\Gamma\|, \tag{66} \end{aligned}$$

where $\lambda_m(\tilde{A}) < 0 = -k$ is the minimum eigenvalue of stable system matrix $\tilde{A}$.

$$\begin{aligned} \dot{\mathcal{V}}_2 &= -\frac{k\|\mathbf{e}\|^2}{2} - \frac{k\|\mathbf{e}\|^2}{2} + \|\mathbf{e}\| \|\Gamma\| + \frac{\|\Gamma\|^2}{2k} - \frac{\|\Gamma\|^2}{2k}, \\ &= -\frac{k\|\mathbf{e}\|^2}{2} - \left\{\frac{k\|\mathbf{e}\|^2}{2} - \|\mathbf{e}\| \|\Gamma\| + \frac{\|\Gamma\|^2}{2k}\right\} + \frac{\|\Gamma\|^2}{2k}, \\ &= -\frac{k\|\mathbf{e}\|^2}{2} - \left\{\frac{\sqrt{k}}{\sqrt{2}}\|\mathbf{e}\| - \frac{\|\Gamma\|}{\sqrt{2k}}\right\}^2 + \frac{\|\Gamma\|^2}{2k}, \\ &\le -\frac{k\|\mathbf{e}\|^2}{2} + \frac{\|\Gamma\|^2}{2k}. \tag{67} \end{aligned}$$

The Lyapunov function $\mathcal{V}_2$ from (64) can be written as

$$\mathcal{V}_2 \le \frac{1}{2}\|\mathbf{e}\|^2 \quad \text{or} \quad \|\mathbf{e}\|^2 \ge 2\mathcal{V}_2. \tag{68}$$

Substituting (68) into (67) yields

$$\dot{\mathcal{V}}_2 \le -k\mathcal{V}_2 + \varphi, \tag{69}$$

where $\varphi = \frac{\|\Gamma\|^2}{2k} > 0$. The solution of (69) is

$$\mathcal{V}_2(t) = \exp^{-kt} \mathcal{V}_2(t_0) + \frac{\varphi}{k}(1 - \exp^{-kt}), \qquad (70)$$

The Lyapunov function $\mathcal{V}_2$ will ultimately converge to a significantly smaller bound given as

$$\mathcal{V}_2 \leq \frac{\varphi}{k}. \qquad (71)$$

Similarly, the error $\mathbf{e}$ will also convergence within a small vicinity of zero with a bound defined as

$$\|\mathbf{e}\| \leq \sqrt{\frac{2\varphi}{k}}, \qquad (72)$$

$\Rightarrow$ as $\mathbf{e}$ converges to a narrow bound around zero, $\hat{\mathbf{x}} \approx \mathbf{x}$. $\square$

Therefore, Theorem 2 shows that with ROM state feedback, one can implement the proposed ROM based design controller to FOM without taking direct feedback from the FOM.

VII. RESULTS AND ANALYSIS

The 3D FE modeling of AMB is carried out using COMSOL Multiphysics. The dimensions and materials used for the designing of AMB in COMSOL are given in Table 1.

TABLE 1. Dimensions and materials of AMB model.

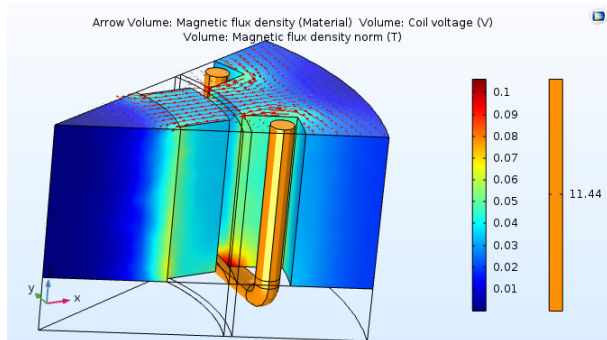| Parameters	Value
Length of AMB	500 mm
Width of AMB	300 mm
Diameter of Coil	3 mm
Number of Turns of Coil	100
Rotational Speed	1200 rpm
Materials	Copper Soft Iron Air

FIGURE 7. Flux density in static simulation.

For extraction of the node matrix, the element matrix and ultimately the entire unreduced model (11) & (12), the software requires two types of simulations to be carried out, the static simulation and the time varying simulation. To achieve static and time varying simulation, full AMB is cut along the width, which can be seen from Figure 7 and 8. The arrows indicate the path of the magnetic flux in this figure.
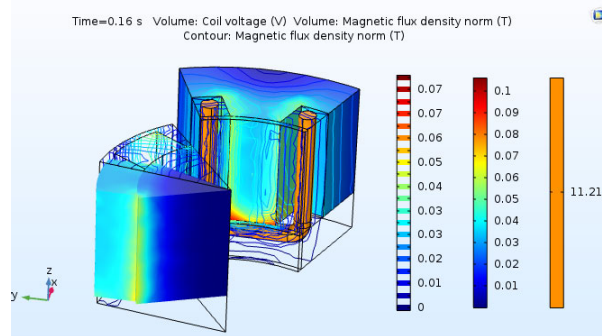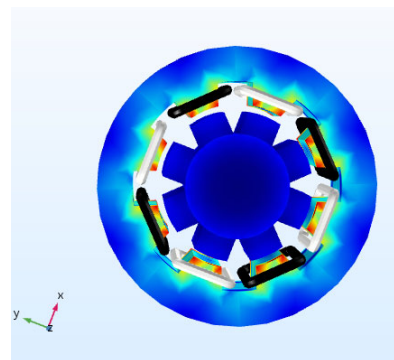
FIGURE 8. Flux density distribution for t=0.16 s.

FIGURE 9. Flux density in full AMB.

In time varying simulation, the model is simulated for $1s$ with a time step of 0.005 s. Figure 8 represents the flux density distribution at an arbitrary chosen time instance $t = 0.16$ s for time varying case. The complete picture of flux density for the full AMB model is shown in Figure 9.

For implementing the proposed control strategy, the system (11) & (12) along with the required system matrices are needed.

For the extraction of the matrices first, the node matrix and element matrix have to be generated. The original model thus obtained in MATLAB is of size 5898. During reduction, due to the large dimension of the Lyapunov equations (17) & (18), it is solved via Matrix Equation Sparse Solver (M.E.S.S.), which is an advanced version of the LyaPack Toolbox for MATLAB [39]. The method described in (20) is one of the ways for solving Lyapunov equations via M.E.S.S. Then, applying balanced truncation on the original model, it is reduced to the order of 20 (i.e., $q = 20$).

Figure 10 shows unit step response of the original and reduced order model of sizes ($q =25, 20, 18, 15,$ and 10). The initial condition is considered zero for this case. It is seen that the curves are matching satisfactorily for reduced models of size 18, 20, and 25. Other reduced models of size 10, 15 differ from the original model curve in transient as well as in steady state stage. Reduced model of size 18 and 20 are matching adequately with the original model curve. But, ROM of size 20 gives slightly better matching with FOM curve. Therefore, the reduced model of size 20 is selected for reduction procedure.
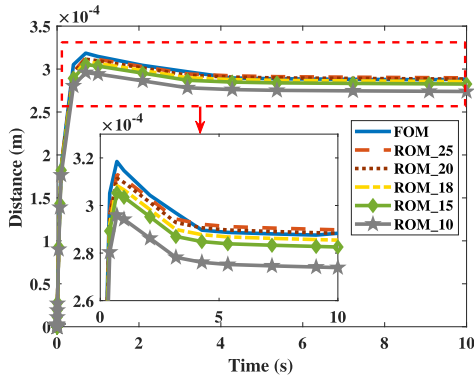
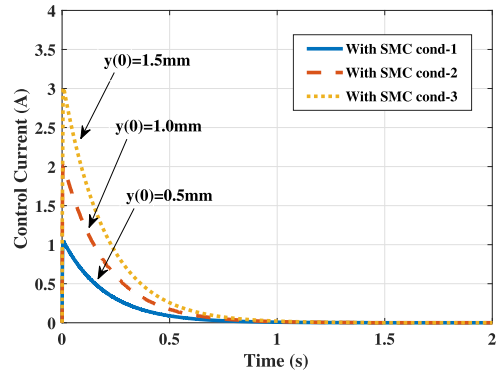**FIGURE 10.** Step response of original and different sizes of reduced model.
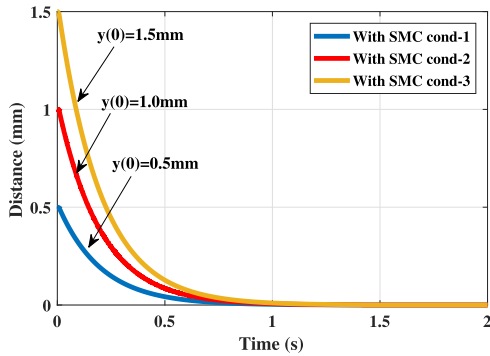

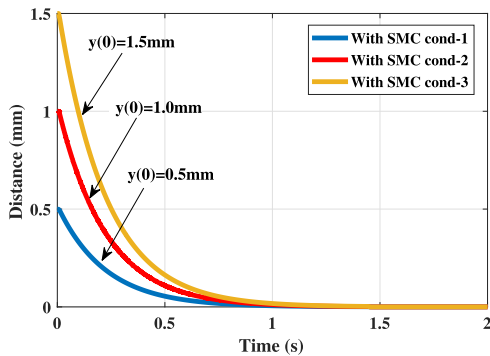**FIGURE 11.** Output displacement of ROM under proposed control (47).

FIGURE 12. Output displacement of FOM under proposed control (47).

The proposed controller (47) is simulated when the rotor is initially displaced from its original position. To validate the controller, different initial displacements y_0 are taken as $y_0 = 0.5$ mm, 1 mm, and 1.5 mm. Under the action of the proposed controller (47), the output response of the reduced order model and the full order model are shown in Figure 11 and 12, respectively, for different initial conditions. The gains of the controller are $c_1 = c_2 = \cdots = c_{19} = 1$ and upper bound of the uncertainties is selected as $\bar{w} = 0.342$. In both of the reduced order model and the full order model, the trajectories are identical. Irrespective of the initial conditions taken as above, the displacement of rotor $y(t)$ identically converges to its original position $y = 0$ within 1 s. Correspondingly, the corrective control input for different

FIGURE 13. Contol Currents with SMC.

initial conditions, as shown in Figure 13, converges to zero at the same time interval within 1 s.

VIII. CONCLUSION

This paper presents a novel approach to design a controller for AMB using reduced order model rather than the original model. FEM modeling of AMB has been discussed, and FEM generated large order model is reduced using balanced truncation. The computational aspects of applying balanced truncation to AMB model is also discussed. The unmodeled dynamics in the reduction process, which is bounded, is taken as bounded uncertainties. Since the original system is of a large order, therefore it is complicated to design the controller for FOM directly.

A sliding mode control law is designed for the ROM to compensate for the effect of unmodeled uncertainties and to regulate the position of the displaced rotor to its origin. The theoretical analysis of the reduced order closed loop system shows the finite time convergence of the ROM states. Then the controller designed for the ROM is applied to the FOM, compensating for the unmodelled uncertainties. The ROM can also be interpreted as an observer for the feedback control design of the FOM. It is proved that the error between the states of FOM and ROM is uniformly ultimately bounded and the error converges to a small vicinity of zero. In the numerical analysis, a 3D simulation of AMB is done using FEM software COMSOL. Model is extracted in MATLAB and reduced to a smaller order model. Various initial conditions are considered for the application of proposed controller to the ROM as well as FOM. The closed-loop performance of ROM with model uncertainties under the action of the proposed control law is satisfactorily consistent with the performance of FOM. Further, the performance result also illustrates the effectiveness of utilizing ROM as an observer for the controller design of full order AMB system.

REFERENCES

[1] H. Bleuler, M. Cole, P. Keogh, R. Larsonneur, E. Maslen, Y. Okada, G. Schweitzer, and A. Traxler, *Magnetic Bearings: Theory, Design, and Application to Rotating Machinery*. Berlin, Germany: Springer-Verlag, 2009.

[2] S. Saha and M. Nabi, "A review on active magnetic bearing and exploitation of parametric model order reduction," in *Proc. IEEE 11th Int. Conf. Ind. Inf. Syst. (ICIIS)*, Roorkee, India, Dec. 2016, pp. 420–425.

[3] C. Peng and Q. Zhou, "Direct vibration force suppression for magnetically suspended motor based on synchronous rotating frame transformation," *IEEE Access*, vol. 7, pp. 37639–37649, 2019.

[4] D. Wajnert, "Comparison of magnetic field parameters obtained from 2D and 3D finite element analysis for an active magnetic bearing," *Solid State Phenomena*, vol. 214, pp. 130–137, Feb. 2014.

[5] B. Polajzer, G. Stumberger, D. Dolinar, and K. Hameyer, "Determination of force and flux linkage characteristics of radial active magnetic bearings," in *Proc. IEEE Region 8 EUROCON Comput.*, vol. 1, Sep. 2003, pp. 442–444.

[6] D. Szypulski, G. Fotyga, and M. Mrozowski, "An enhanced reduced basis method for wideband finite element method simulations," *IEEE Access*, vol. 7, pp. 60877–60884, 2019.

[7] P. K. Biswas and S. Banerjee, "ANSYS based fem analysis for three and four coil active magnetic bearing-a comparative study," *Int. J. Appl. Sci. Eng.*, vol. 11, no. 3, pp. 277–292, 2013.

[8] A. Pilat, "Analytical modeling of active magnetic bearing geometry," *Appl. Math. Model.*, vol. 34, no. 12, pp. 3805–3816, 2010.

[9] M. Jungwirth, D. Hofinger, and H. Weinzierl, "A comparison of model order reduction methods used in different FE software tools," in *Proc. 11th Int. Conf. Therm., Mech. Multi-Phys. Simulation, Exp. Microelectron. Microsyst. (EuroSimE)*, Apr. 2010, pp. 1–5.

[10] Y. Le and K. Wang, "Design and optimization method of magnetic bearing for high-speed motor considering eddy current effects," *IEEE/ASME Trans. Mechatronics*, vol. 21, no. 4, pp. 2061–2072, Aug. 2016.

[11] A. C. Antoulas, *Approximation of Large-Scale Dynamical Systems*. Philadelphia, PA, USA: SIAM, 2005.

[12] U. Baur, P. Benner, and L. Feng, "Model order reduction for linear and nonlinear systems: A system-theoretic perspective," *Arch. Comput. Methods Eng.*, vol. 21, no. 4, pp. 331–358, 2014.

[13] P. Benner, K. Willcox, and S. Gugercin, "A survey of projection-based model reduction methods for parametric dynamical systems," *SIAM Rev.*, vol. 57, no. 4, pp. 483–531, 2011.

[14] M. Kiani, H. Salarieh, A. Alasty, and S. M. Darbandi, "Hybrid control of a three-pole active magnetic bearing," *Mechatronics*, vol. 39, pp. 28–41, Nov. 2016.

[15] C. Peng, J. Fang, and X. Xu, "Mismatched disturbance rejection control for voltage-controlled active magnetic bearing via state-space disturbance observer," *IEEE Trans. Power Electron.*, vol. 30, no. 5, pp. 2753–2762, May 2015.

[16] M. Hutterer, M. Hofer, and M. Schrödl, "Decoupled control of an active magnetic bearing system for a high gyroscopic rotor," in *Proc. IEEE Int. Conf. Mechatronics (ICM)*, Mar. 2015, pp. 210–215.

[17] A. A. Abouelsoud and A. M. Mohamed, "Adaptive controller for stabilisation of rotational motion of a vertical shaft magnetic bearing," *Int. J. Model., Identificat. Control*, vol. 23, no. 2, pp. 154–163, 2015.

[18] S.-Y. Chen and M.-H. Song, "Energy-saving dynamic bias current control of active magnetic bearing positioning system using adaptive differential evolution," *IEEE Trans. Syst., Man, Cybern. Syst.*, vol. 49, no. 5, pp. 942–953, Apr. 2017.

[19] Y. Zheng, N. Mo, Y. Zhou, and Z. Shi, "A model-free control method for synchronous vibration of active magnetic bearing rotor system," *IEEE Access*, vol. 7, pp. 79254–79267, 2019.

[20] A. Bonfitto, L. C. Molina, A. Tonoli, and N. Amati, "Offset-free model predictive control for active magnetic bearing systems," *Actuators*, vol. 7, no. 3, p. 46, 2018.

[21] M.-J. Jang, C.-L. Chen, and Y.-M. Tsao, "Sliding mode control for active magnetic bearing system with flexible rotor," *J. Franklin Inst.*, vol. 342, no. 4, pp. 401–419, 2005.

[22] B. D. Hoang, "Second order sliding mode control design for active magnetic bearing system," in *AETA 2015: Recent Advances in Electrical Engineering and Related Sciences*. Cham, Switzerland: Springer, 2016, pp. 519–529.

[23] A. Niemann, G. van Schoor, and C. du Rand, "A self-sensing active magnetic bearing based on a direct current measurement approach," *Sensors*, vol. 13, no. 9, pp. 12149–12165, 2013.

[24] X.-D. Yang, H.-Z. An, Y.-J. Qian, W. Zhang, and M.-H. Yao, "Elliptic motions and control of rotors suspending in active magnetic bearings," *J. Comput. Nonlinear Dyn.*, vol. 11, no. 5, 2016, Art. no. 054503.

[25] B. Polajzer, G. Štumberger, J. Ritonja, and D. Dolinar, "Linearization of radial force characteristic of active magnetic bearings using finite element method and differential evolution," in *Magnetic Bearings, Theory and Applications*. Rijeka, Croatia: InTech, 2010.

[26] M. A. Bazaz and S. Janardhanan, "Two-step reduction procedure for parametric transient electromagnetic computations," in *Proc. Int. Conf. Modeling, Identificat. Control (ICMIC)*, Jun. 2012, pp. 1204–1209.

[27] M. U. Nabi, S. V. Kulkarni, and V. R. Sule, "Novel modeling and solution approach for repeated finite-element analysis of eddy-current systems," *IEEE Trans. Magn.*, vol. 40, no. 1, pp. 21–28, Jan. 2004.

[28] S. Gugercin and A. C. Antoulas, "A survey of model reduction by balanced truncation and some new results," *Int. J. Control*, vol. 77, no. 8, pp. 748–766, 2004.

[29] S. Gugercin, D. C. Sorensen, and A. C. Antoulas, "A modified low-rank Smith method for large-scale Lyapunov equations," *Numer. Algorithms*, vol. 32, no. 1, pp. 27–55, 2003.

[30] P. Benner, P. Kürschner, and J. Saak, "A reformulated low-rank ADI iteration with explicit residual factors," *PAMM*, vol. 13, no. 1, pp. 585–586, 2013.

[31] P. Benner and E. S. Quintana-Ortí, "Solving stable generalized Lyapunov equations with the matrix sign function," *Numer. Algorithms*, vol. 20, no. 1, pp. 75–100, 1999.

[32] P. Benner, J. Claver, and E. Quintana-Ort, "Efficient solution of coupled Lyapunov equations via matrix sign function iteration," in *Proc. 3rd Portuguese Conf. Autom. Control (CONTROLO)*, 1998, pp. 205–210.

[33] P. Benner, P. Kürschner, and J. Saak, "Improved second-order balanced truncation for symmetric systems," in *Proc. 7th Vienna Int. Conf. Math. Modeling (MATHMOD)*, 2012, pp. 758–762.

[34] P. Benner, A. Cohen, M. Ohlberger, and K. Willcox, *Model Reduction and Approximation: Theory and Algorithms*, vol. 15. Philadelphia, PA, USA: SIAM, 2017.

[35] K. Zhou, J. C. Doyle, and K. Glover, *Robust and Optimal Control*, vol. 40. Upper Saddle River, NJ, USA: Prentice-Hall, 1996.

[36] P. Guha, "Reduced order modeling and control of distributed parameter systems," Ph.D. dissertation, Indian Inst. Technol. Delhi, New Delhi, India, May 2013.

[37] S. P. Bhat and D. S. Bernstein, "Finite-time stability of continuous autonomous systems," *SIAM J. Control Optim.*, vol. 38, no. 3, pp. 751–766, Jan. 2000.

[38] S. M. Amrr, A. Banerjee, and M. Nabi, "Robust attitude control of rigid spacecraft based on event-triggered approach with anti-unwinding," in *Proc. IEEE 5th Indian Control Conf. (ICC)*, New Delhi, India, Jan. 2019, pp. 510–515.

[39] J. Saak, M. Köhler, and P. Benner, "MM.ESS-1.0.1—The matrix equations sparse solvers library," Tech. Rep., 2016. [Online]. Available: https://doi.org/10.5281/zenodo.50575

SUDIPTA SAHA (S'19) received the bachelor's degree in electrical engineering from the West Bengal University of Technology (WBUT), Kolkata, India, in 2012, and the M.Tech. degree in mechatronics and robotics from the School of Mechatronics and Robotics, IIEST, Shibpur, India, in 2015. He is currently pursuing the Ph.D. degree with the Control and Automation Group, Department of Electrical Engineering, IIT Delhi (IITD), India. His research interests include model-order reduction and sliding mode control using reduced-order models.

SYED MUHAMMAD AMRR (S'18) received the bachelor's degree in electrical engineering and the master's degree in instrumentation and control from the Department of Electrical Engineering, Aligarh Muslim University (AMU), Aligarh, India, in 2014 and 2016, respectively. He is currently pursuing the Ph.D. degree with the Control and Automation Group, Department of Electrical Engineering, IIT Delhi (IITD), New Delhi, India. His research interests include nonlinear control, sliding mode control, robust control, spacecraft attitude control, renewable energy, and power electronics.

MASHUQ UN NABI (M'10) received the B.E. degree in electrical engineering from Jadavpur University, Kolkata, India, in 1997, the M.Tech. degree in electrical engineering from IIT Kanpur (IITK), India, in 1999, and the Ph.D. degree from IIT Bombay (IITB), India, in 2004. He joined the Department of Electrical Engineering, IIT Delhi (IITD), in 2005 where he is currently an Associate Professor. His research interests mainly include reduced-order modeling (model-order reduction), optimal control, sliding mode control, neuro-fuzzy control, and computational electromagnetics.

ATIF IQBAL (M'08–SM'11) received the B.Sc. (Hons.) and M.Sc. Engineering degrees in power system and drives from Aligarh Muslim University (AMU), Aligarh, India, in 1991 and 1996, respectively, and the Ph.D. degree from Liverpool John Moores University, Liverpool, U.K., in 2006. He is currently an Associate Professor of electrical engineering with Qatar University, Doha, Qatar, and a Former Full Professor of electrical engineering with AMU. He has been a Lecturer with the Department of Electrical Engineering, AMU, since 1991, where he has served as a Full Professor, until August 2016. He has published widely in international journals and conferences his research findings related to power electronics and renewable energy sources. He has authored/coauthored more than 350 research papers and one book and three chapters in two other books. He has supervised several large R&D projects. His research interests include modeling and simulation of power electronic converters, control of multiphase motor drives, and renewable energy sources. He is also a Fellow of IET, U.K., and IE, India. He was a recipient of the Outstanding Faculty Merit Award AY (2014–2015) and the Research Excellence Award at Qatar University. He was a recipient of the Maulana Tufail Ahmad Gold Medal for standing first at B.Sc. Engg. Exams, in 1991, from AMU. He received best research papers awards at IEEE ICIT-2013, IET SEISCON-2013, and SIGMA 2018. He is also an Associate Editor of the IEEE TRANSACTIONS ON INDUSTRY APPLICATIONS and IEEE ACCESS and the Editor-in-Chief of the *Journal of Electrical Engineering* (i-manager).

• • •